Available online at www.sciencedirect.com
ScienceDirect
Applied Radiation and Isotopes 65 (2007) 419–427
Applied Radiation and Isotopes
www.elsevier.com/locate/apradiso

Influence of inlet positions on the flow behavior inside a photoreactor using radiotracers and colored tracer investigations

Rubens M. Moreira[a], Amenônia M.F. Pinto[a], Raphaël Mesnier[b], Jean-Pierre Leclerc[b,*]

[a]*Center for Development of Nuclear technology, Belo Horizonte, Brazil*
[b]*Laboratoire des Sciences du Génie Chimique de Nancy, CNRS-ENSIC, 1, rue Grandville B.P. 20451, 54001 Nancy Cedex, France*

Received 3 March 2006; received in revised form 14 September 2006; accepted 20 September 2006

Abstract

The influence of the inlet positions on the flow behavior inside a photoreactor has been studied using colored tracer and radiotracer investigations. The photoreactor for water disinfection is a tubular reactor inside which UV emitting lamps are placed. The key to its good performance is a combination of optimum irradiation dose and fluid residence time distributions (RTD). The inlet system is one of the better possibilities of controling the fluid RTD. Three configurations have been tested. In the first step, colored tracer experiments help us to raise the mean trends of the flow behavior for the different configurations. When the inlet is located at the central bottom of the reactor, the flow is closed to a perfect mixing whereas lateral inlets lead to a plug flow with axial dispersion behavior. RTD measurements using radiotracer was carried out in a wide range of flowrates. The axial dispersion coefficient increases linearly with the Reynolds number. It is lower when the lateral inlet is divided in three inlets uniformly distributed around the bottom of the reactor. This paper shows the usefulness of radioactive isotopes as tracers in the field of wastewater treatment.

Keywords: Photoreactor; Residence time distribution; Radioactive isotope; Tracers; Water treatment

1. Introduction

UV radiation is quite effective in pathogen inactivation and is even more effective against viral organisms than chlorine (Qualls and Johnson, 1985), with a broad spectrum of effluents. It is a relatively simple method that does not require stocking, transport and chemical manipulations, qualified personnel to deal with it, and does not generate residues. Besides, the risk of an overdose does not impact receiving watercourses (USEPA, 1986).

Research on this technique has been resumed (Oliver and Cosgrove, 1975). Initial results on fecal coliform inactivation in pilot scale proved successful, and this prompted other investigators to apply the technology to real-scale flow (Scheible and Bassell, 1981).

The bactericide action is related to the UV absorption by DNA molecules and the consequent formation of pyrimidines (thymine and cytosine) dimers, the maximum yield being reached at the 260 nm wavelength (USEPA, 1986). These dimers inhibit DNA replication, leading to the death of the cell. In the case of viruses, inactivation stems from uracil, instead of thymine, dimerization. The main sources of UV radiation at the above wavelength are commercial low-pressure mercury lamps whose energy peak is at 254 nm (about 85%), and their quartz bulbs allow the transmission of 93% of the intensity. New lamps are being made available, such as the low pressure and high output (LPHO), which raise the power and lower the cost (Alves, 2003). Experiments conducted by Liu et al. (2002) have shown that the UV doses typically used in sewage disinfection (less than 500 mW s/cm^2) do not result in byproduct formation.

To illustrate the efficiency of the method and the broad spectrum of applications, Table 1 summarizes the results from several studies related to secondary and tertiary effluent disinfection by means of UV radiation incident upon total and fecal coliforms, as well as *Escherichia coli* indicators. The last line in the table gives results obtained with the industrial reactor presented in this paper.

*Corresponding author. Tel.: +33 3 83 17 50 66; fax: +33 3 83 327 308.
E-mail address: leclerc@ensic.inpl-nancy.fr (J.-P. Leclerc).

0969-8043/$ - see front matter © 2006 Elsevier Ltd. All rights reserved.
doi:10.1016/j.apradiso.2006.09.012

Table 1
Results from UV disinfection of total coliforms, fecal coliforms and *E. coli*

Reference	Dosis (mW s/cm^2)	Suspended solids (mg/l)	Transmittance (%)	Efficiency (log)	Effluent
Andreadakis et al. (1999)	30	20	38	2.3	Secondary
Castro Silva (2001)	41	64	—	4.7	UASB reactor
Castro Silva (2001)	21	46	—	4.9	Percolating biologic filter
Gonçalves et al. (2001b)	59	26	41	4.5	Submersed aerated biofilter
Gonçalves et al. (2001b)	21	16	39	3.8	Tertiary filter
Janex et al. (1998)	37	17–85	48–60	3.0	Secondary
Qualls and Johnson (1985)	26	32	—	3.1	Activated sludge
Savoye et al. (2001)	25	81	45	2.3	Activated sludge
Alves (2003)	22	75	38	3.1	UASB reactor
	22	19	56	3.3	Percolating biologic filter
	22	102	18	2.6	Maturation pond

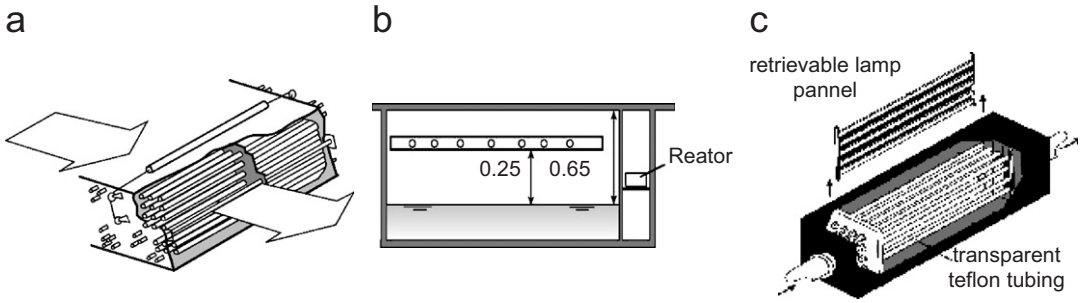

Fig. 1. Sketch of the three main photoreactor types (Chernicharo et al., 2001).

Photocatalytic reactors have also been intensively studied. They contain semi-conductor catalysts such as TiO_2 that efficiently generate the highly reactive $^{\bullet}OH$ free radicals, which are highly toxic towards microorganisms and can drive oxidation processes suitable for the abatement of organic contaminants in water. Some of these reactors make profit of sunlight for this purpose; use is made of the near-UV part of the solar spectrum ($\lambda < 380$ nm) to photoexcite the catalyst (Malato et al., 2002). Working with a pilot-scale-fluidized photocatalytic reactor handling 46 l/min, Kabir et al. (2003) have found that it is capable of degrading 84% of *E. coli* within 80 min compared with 77.3% by using UV only.

However, these photocatalytic processes are highly influenced by the variations of parameters such as light intensity, catalyst concentration, initial bacterial concentration, and the presence of organic matter. These parameters must be carefully adjusted in order to optimize and stabilize the inactivation yield, and this is a handicap in the case of simple treatment plants devised to be operated by non-specialized personnel.

Water disinfection can be carried in different photoreactors (Chernicharo et al., 2001), as shown in Fig. 1:

(a) Lamps placed inside the liquid.
(b) Lamps backed with reflectors placed above the liquid.
(c) Lamps external to the fluid that flows inside transparent tubing.

Photoreactors designed for wastewater disinfection often consist of a set of lamps mounted inside an encased space, in contact with the effluent, which flows either parallel or transversally to them. Besides the characterization of the disinfection kinetics, the influence of suspended solids and the operational costs in such photoreactors, a basic requirement is the evaluation of its hydrodynamic behavior. Due to its decisive influence on the reaction yield, this last item is still a theme for ongoing investigation and optimization. The intensity of the radiation inside the reactor decreases exponentially with the distance from the lamps according to Beer's law. Hence under ideal conditions, plug flow should be attained, assisted by a satisfactory amount of radial turbulence, so that each fluid element would receive the same radiation dose during its transit through the reactor. Dead zones and preferential paths should be avoided since they result in a low efficiency of the power of the lamps, which represents the largest component of the UV disinfection implantation and operation costs. The hydrodynamic behavior of different kinds of photoreactors has been previously studied by several investigators (Kreft et al., 1986; Qualls and Johnson, 1985; Gonçalves et al., 2001a; Legentilhomme and Legrand, 1995; Pruvost et al., 2000;

Pruvost et al., 2001; Pruvost et al., 2002). Most of the studied reactors are made with one lamp placed inside a narrow tube. In this case, the use of a tangential inlet induces a swirling flow, which gives a better radial dispersion (Legentilhomme and Legrand, 1995; Pruvost et al., 1999). Sahle-Demessie et al. (2003) measured the residence time distributions (RTD) of the gas flow in a stirred annular photoreactor. They compared qualitatively RTD and computational fluid dynamic's simulations with and without fan. The use of axial or mixed flow stirred makes the RTD curve narrow. Qualls and Johnson (1985) showed that high dispersion of the RTD may dramatically affect the efficiency. Recently Pruvost et al. (2000, 2001, 2002) did a remarkable work on flow characterization in a Swirling annular photoreactor using the Lagrangian trajectory model (Pruvost et al., 2002), Particule Image Velocimetry (Pruvost et al., 2000; pruvost et al., 2001). These methods give detailed information about local velocities, which cannot be obtained with the RTD measurements. However, they are optical methods which necessitate having a transparent pilot. Moreover, the experiments are time-consuming and post-treatment is not straightforward. To get the benefice of these accurate and detailed measurements, it is also necessary to repeat the measurement when changing one part of the reactor having a strong effect on the flow behavior. Nevertheless, the profit of these methods is unquestionable when the design of the reactor is definitely stated.

The objective of this work is to study the influence of the inlets position on the flow behavior of a new photoreactor using radiotracer experiments. The interpretation of the radiotracer experiment will be validated with the help of visualizations.

2. Experimental

The reactor tested in the present study and its dimensions are shown in Fig. 2. It is well-adapted in developing countries because it has a very simple design and can be easily built in any plain workshop with ready-to-find materials; the outer casing can consist of a PVC tube, painted in black, to retain the internal radiation. For a given flowrate, and if configuration of the photoreactor is fixed, the inlet system can be adapted to obtain the requested flow behavior. A transparent pilot (see Figs. 3 and 4) at the same scale of the real reactor has been used to study the flow behavior. Three configurations of the inlet system have been proposed to obtain different RTD:

- Configuration 1: One central bottom inlet.
- Configuration 2: One lateral inlet.
- Configuration 3: Three lateral inlets around the bottom of the reactor for which the global flowrate is divided in three equal flowrates.

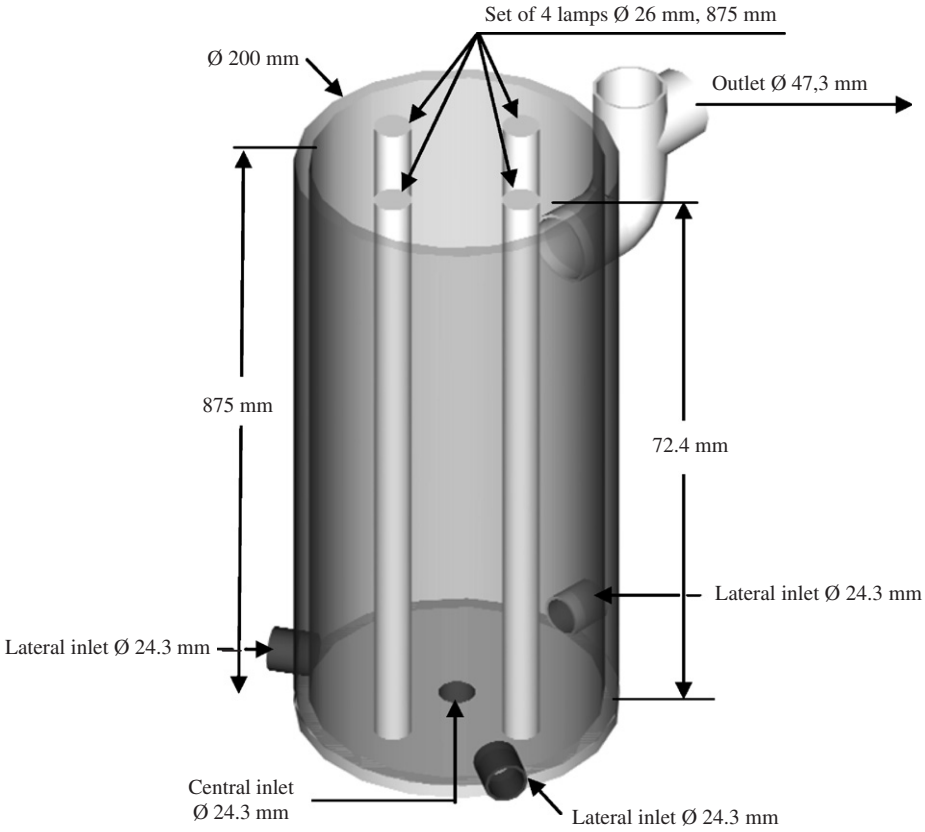

Fig. 2. Scheme of the photoreactor with four vertical lamps and upward flow.

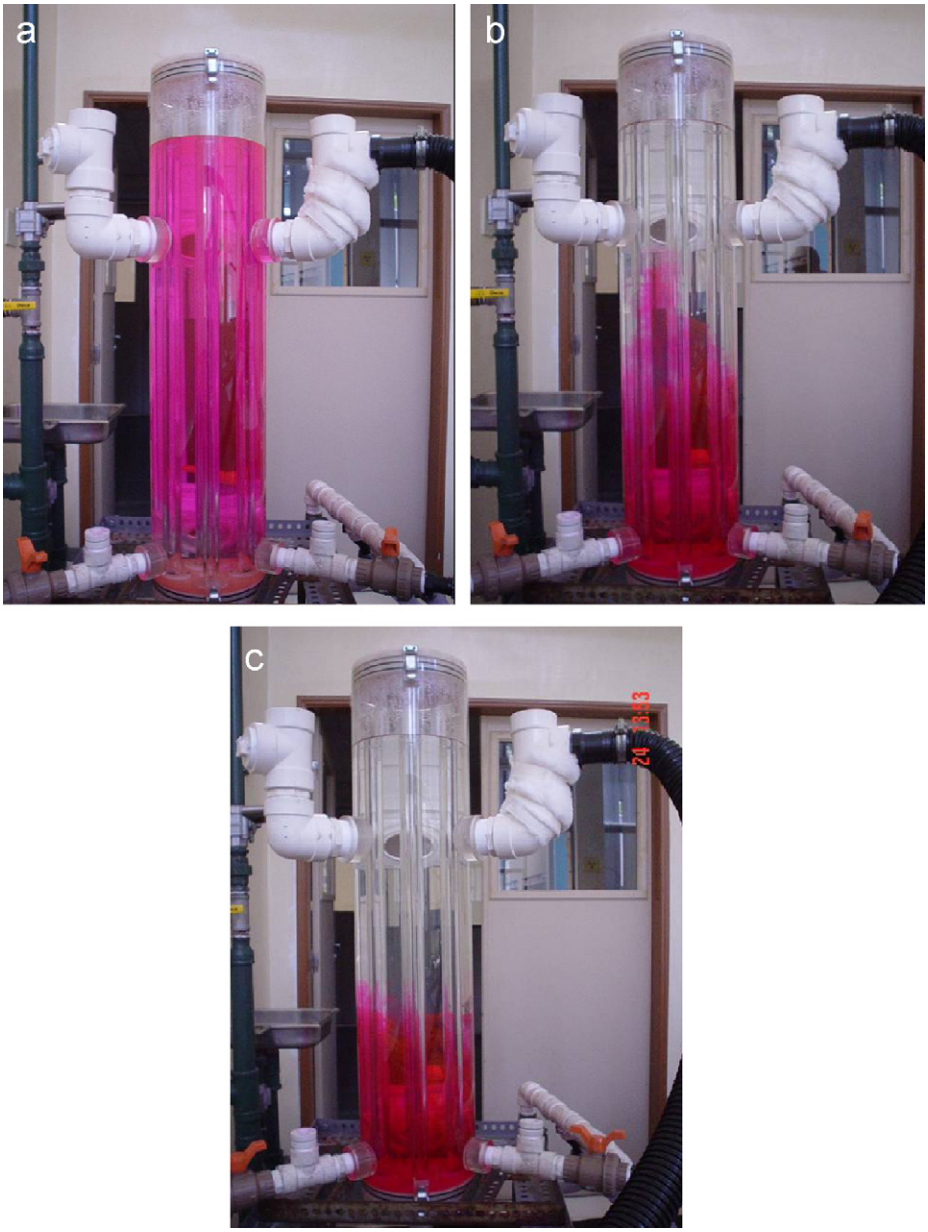

Fig. 3. Visualization using colored tracer in the pilot 5 s after the injection: (a) configuration 1 : 1 central inlet, (b) configuration 2 : 1 lateral inlet, (c) configuration 3, 3 lateral inlets. The several inlets are clearly visible at the bottom of the pilot. The event in the exit located after the elbow, maintains constant the water level inside the reactor.

During the first series of experiment Rhodamine WT dye solution was used to visualize the internal flow. Several photos were taken every 5 s to analyze the dispersion of the colored tracer inside the reactor. During the second series of experiment, a pulse of radiotracer was injected manually at the inlet with a syringe. The inlet signal was recording continuously and all the interpretations were done taking into account the inlet signal. The radiotracer used in the study was ^{113m}In ($E_\gamma = 0.14$ MeV). It is obtained using a radionucleide generator of the kind ^{113}Sn/^{113m}In. ^{113m}In has a half-life of 100 min, which is long enough to carry out the measurement that lasts less than 10 min. The maximum activity used in these experiments was 1 mCi ($\approx$37 MBq). The ^{113m}In in the eluent HCl 0.05 N acts as a marker of water. The radiotracer emitting γ-radiation was injected as a pulse function at the inlet of the studied system with a pressured injection system. The scintillation probe, placed at the inlet and the outlet, detects the gamma radiation as a time function. Since the counting rate is directly proportional to the concentration of the radiotracer in the flowing stream where the probes are placed, the curves give direct access to the RTD. The detection system (FORCE Technology) was composed of several hermetic detectors (IC-2N2-WT-50 m) connected with long polyurethane-shielded wires to a compact processing data unit (IC-GDP), at which was coupled a computer RS-232 communication port. The hermetical detectors are composed of $2'' \times 2''$ NaI(TI) scintillation crystals. The shielding collimation was done to minimize, as much as possible, the effect of radiation from the inside of the reactor.

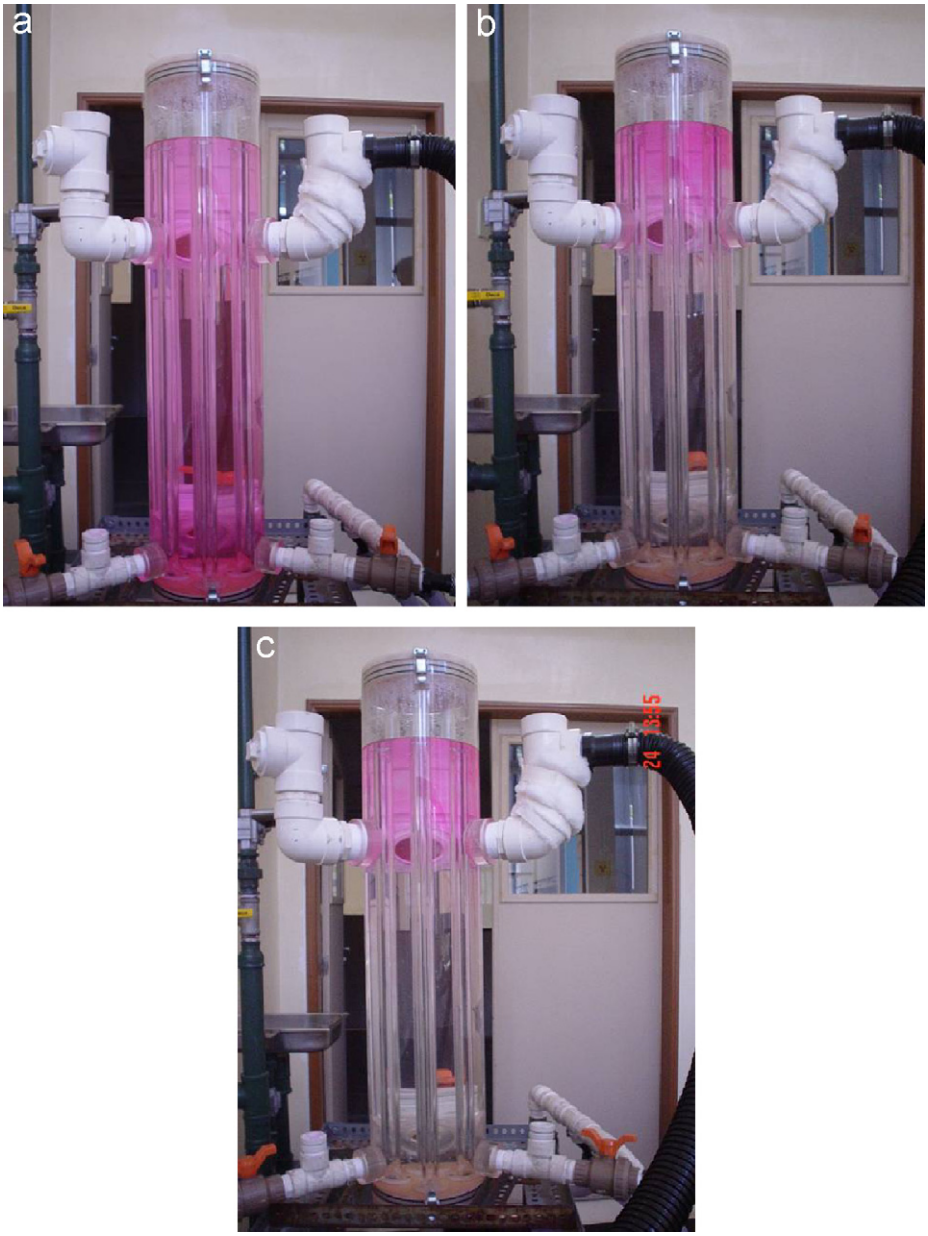

Fig. 4. Visualization using colored tracer, 90 s after the injection: (a) configuration 1 : 1 central inlet, (b) configuration 2 : 1 lateral inlet, (c) configuration 3, 3 lateral inlets.

3. Data analysis, results and discussion

The study was conducted in three steps:

- qualitative visualization of the flow using colored tracer,
- qualitative analysis of the RTD curves using the first moments,
- simulation of the RTD curves using compartment models.

3.1. Colored tracer investigations and mean trends of the flow

RTD remains an interesting method to derive simple hydrodynamic models for complex industrial systems. The interpretation of RTD measurements by use of a "compartment model" is based on both the analysis of the RTD curve and the physical information about the process itself. If the approach was merely based on mathematical fitting of an experimental RTD curve, it may lead to models without correct physical meaning. The additional use of the physical aspects of the process itself results in a wider knowledge, which cannot be generated by mathematical treatment alone (Claudel et al., 2003). To overcome this problem, colored tracer visualization was carried out with the help of a transparent pilot to increase the knowledge of the process before the interpretation of the RTD curves. Figs. 3 and 4 represent, respectively, the photo taken after 5 and 90 s of experiment for the three configurations (a, b, c). When the inlet is located in the center of the bottom of

the reactor (photo a), the tracer is instantaneously dispersed in the whole reactor as shown in Fig. 3a. The colored intensity decreased slowly, homogeneously, in the reactor and after 90 s the reactor was still entirely colored by the residual dyes. This suggests that flow behavior was closed to the perfect mixing. Visual observation in the few first seconds showed a jet flow effect at the inlet that suggested the presence of a small plug flow volume induced by this jet. For the two other configurations, the flow behavior was closer to a plug flow with some dispersion. The tracer goes progressively from the bottom to the top with some dispersion. The dispersion seems to be much less important when the inlet is divided in three parts. These visual observations will be used later for the choice of the compartment model.

3.2. Radiotracer experiments and preliminary interpretation of the RTD

The RTD is a chemical engineering concept introduced by Danckwerts (1953). It has been described in a multitude of scientific papers (Dudukovic, 1986; Levenspiel, 1999, etc.) and applied for various industrial processes.

$$E(t) = \frac{C_{out}(t)}{\int_0^\infty C_{out}(t)\,dt}, \quad C_{out}(t) = \int_0^t C_{in}(x)E(t-x)\,dx.$$

(For a constant flow rate Q and uniform speed of fluid in the inlet and outlet sections) (1)

$E(t)$ is, by definition (see Eq. 1), the impulse response (or RTD) of the system. It is easily obtained by dividing the concentration $C_{out}(t)$ by the total surface under the curve. In the case of a non-instantaneous injection, whose function is in the form of $C_{in}(t)$, the curve $C_{out}(t)$ obtained on the outlet is equal to the product of the convolution of $C_{in}(t)$ by the impulse response $E(t)$.

The first moment of the experimental RTD gives the mean residence time of the material inside the studied process. The second moment leads to an estimate of the dispersion, which is representative of the flow behavior. The first moment is especially useful when the presence of dead volume and shortcuts are expected. For the studied configuration, the outlet is located down to the level of the reactor which lets us suspect a possible dead volume when the Reynolds number is too low. Moreover, it is not obvious whether the fluid is homogeneously distributed around the area of the inlet pipe. Because of this, the first moments of the RTD curves have been estimated for the three configurations and for a large range of flowrates.

The visualizations showed that the central inlet induces a perfect mixing flow, which is not adapted for the photoreactor. Because of this, few radiotracers experiments have been conducted with this configuration. Fig. 5 shows the mean residence time obtained from the experimental data and the space-time volume obtained with the geometrical data of the reactor. The mean residence time in the photoreactor is obtained by the difference between

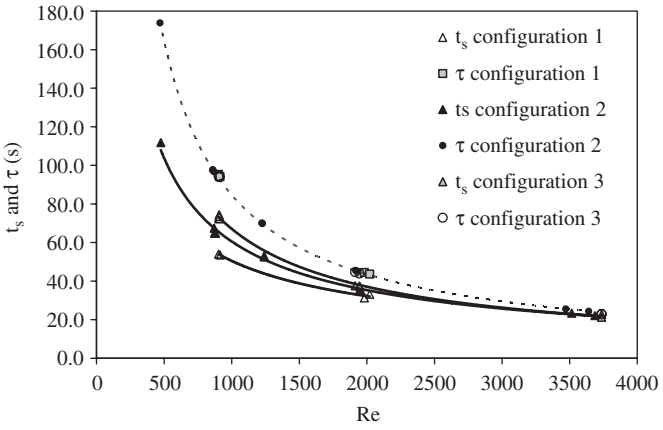

Fig. 5. Mean residence time and space-time volume versus Reynolds number for the three configurations.

the first moment of the tracer outlet concentration versus time (μ_1 outlet) and the first moment of the tracer inlet concentration versus time (μ_1 inlet). Several methods may be used for this estimation and the accuracy is different from one to another (Stegowski, 1993). However, in the present case, the simplest method is accurate enough to calculate the stagnant volume. The data have been plotted as a function of the Reynolds number based on the internal diameter of the reactor as given by relation 2

$$Re = \frac{Ud\rho}{\mu}, \quad (2)$$

where U is the linear velocity inside the reactor, d the internal hydraulic diameter, ρ the density and μ the viscosity of the fluid. The flowrate was changed to test several values of the Reynolds number.

For all configurations, the difference between the space-time volume and the mean residence time decreases with the Reynolds number. When Reynolds number reaches the turbulent zone, the difference becomes smaller. The configuration with three lateral inlets allows to obtain better results, even if a difference remains between the space-time volume and the mean residence time.

The percentage of stagnant volume has been estimated for the different configuration versus Reynolds number (see Fig. 6). Configuration 3 with three lateral inlet gives, as expected, better results since the flow is well distributed inside the reactor. It should be pointed out that one part of the stagnant volume is clearly due to the chosen configuration in which the outlet is located down to the water level surface for other technological considerations. However, the adapted configuration using a reasonable Reynolds number allows overcoming this problem.

3.3. Modeling of the RTD

The moments of the RTD provide only global information that are not sufficient for an accurate description of the flow behavior. Better understanding of the complex processes can be obtained by simulation of the experimental

RTD using compartment models (Levenspiel, 1999). Depending of the complexity of the system, fuzzy logic methods allow proposing a multiple parameters model with good confidence (Claudel et al., 2003).

For each configuration, a model has been proposed based on colored tracer experiments and the parameters have been determined by fitting experimental and simulated RTD curves. The simulations and the adjustment of the parameters have been obtained using DTSpro software (Leclerc et al., 1995, 2000). For the first configuration, the flow behavior was modeled by a small plug flow reactor representing the jet effect followed by a perfect mixing cell. The operating and model parameters obtained for the whole experiments of the three configurations are given in Table 2. Fig. 7 represents the scheme of this model, the model has only two parameters, the mean residence time in the plug flow reactor τ_{pf} and the mean residence time in the perfect mixing cell τ_{pmc}. Fig. 8 illustrates the good agreement obtained between the proposed model and the experimental data. Similar agreement has been obtained with the whole set experiments. The obtained parameters are meaningful since volume of the plug flow part is increasing from around 1.5 l (i.e. mean residence time of 3–4 s) for the lower Reynolds number ($Re = 900$ in the reactor, $Re = 11{,}000$ in the inlet pipe) to around 31 (i.e. mean residence time of 6–7 s) for the higher one ($Re = 2000$ in the reactor, 24,500 in the inlet pipe), the volume is consistent with the visual observation and it is known that the jet increases with the Reynolds number.

For the lateral inlet configurations, the plug flow with the axial dispersion model has been chosen, thanks to the visual observations. This model has also only two parameters, the mean residence time and the Peclet number defined by relation 3:

$$Pe = \frac{UL}{D}, \tag{3}$$

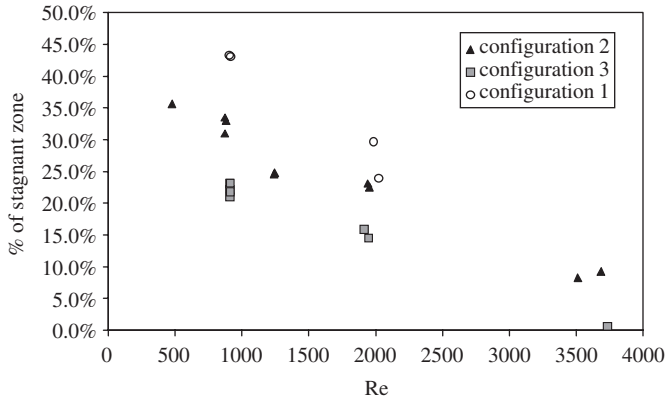

Fig. 6. Percentage of stagnant volume versus Reynolds number for the three configurations.

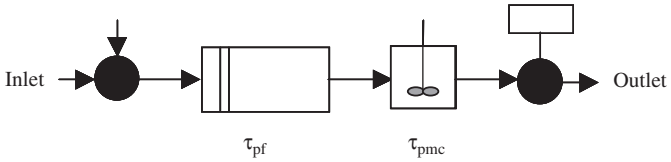

Fig. 7. Compartment model selected for the first configuration.

Table 2
Operating and modeling parameters

Configuration	Q (l/s)	u (m/s)	Re	μ_1 inlet (s)	μ_1 outlet (s)	t_s (s)	τ (s)	Pe	Stagnant zone (%)	D (m^2/s)	τ_{pf}(s)	τ_{mc}(s)
2	0.1122	0.00405	476	194.89	306.72	111.8	173.8	5	35.7	0.000587		
2	0.2052	0.00741	870	156.24	223.72	67.5	97.7	6	31.0	0.000894		
2	0.2058	0.00743	873	80.28	145.1	64.8	97.5	5	33.5	0.00108		
2	0.20748	0.00749	880	39.29	104.08	64.8	96.7	6	33.0	0.000904		
2	0.2922	0.0106	1239	68.51	121.36	52.8	70.1	6	24.6	0.000128		
2	0.2932	0.0106	1244	68.74	121.28	52.5	69.8	6	24.8	0.00128		
2	0.4579	0.0165	1942	87.05	122	35	45.4	6	23.1	0.002		
2	0.4612	0.0167	1956	73.75	108.73	35	45.1	7	22.5	0.00172		
2	0.8288	0.0299	3515	51.75	75.19	23.4	25.5	6	8.2	0.00361		
2	0.8693	0.0314	3687	91.18	113.28	22.1	24.3	7	9.3	0.00325		
1	0.4673	0.0169	1982	95.48	126.74	31.3	44.5		29.7	—	4	18
1	0.4766	0.0172	2021	197.34	230.5	33.2	43.6		23.9	—	3	16
1	0.2129	0.00769	903	180.1	234.09	54	95.3		43.3	—	7	41
1	0.2155	0.00778	914	81.64	135.18	53.5	94.1		43.1	—	6	39
3	0.2139	0.00772	907	73.93	147.24	73.3	94.2	8	22.1	0.000699		
3	0.2133	0.0077	905	174.79	247.38	72.6	94.4	10	23.1	0.000558		
3	0.2139	0.00772	907	38.93	113.34	74.4	94.2	9	21.0	0.000621		
3	0.2142	0.00774	908	176.33	248.57	72.2	94	12	23.2	0.000467		
3	0.2142	0.00774	908	96.14	169.63	73.5	94	11	21.8	0.000509		
3	0.4588	0.0166	1946	91.41	128.92	37.5	43.9	11	14.6	0.00109		
3	0.4511	0.0163	1913	125.68	163.22	37.5	44.6	9	15.9	0.00131		
3	0.881	0.0318	3737	37.95	60.67	22.7	22.9	11	0.7	0.00209		
3	0.881	0.0318	3737	49.37	70.63	21.3	22.9	9	7.0	0.00256		

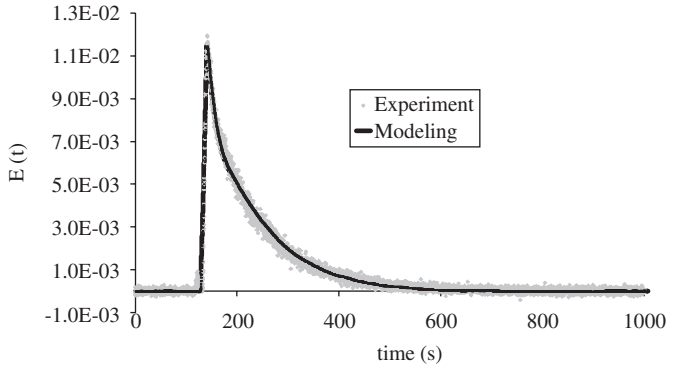

Fig. 8. Comparison between experimental outlet tracer concentration curve and simulation for the configuration 1, central bottom inlet.

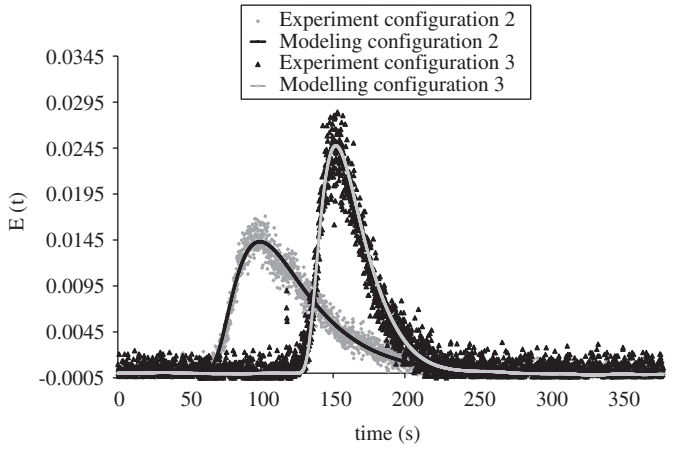

Fig. 9. Comparison between experimental outlet tracer concentration curve and simulation for the configuration 2, one lateral inlet, and configuration 3, three lateral inlets.

where U is the linear velocity in the reactor, L the length of the reactor and D the axial dispersion coefficient. Fig. 9 shows an example of the good agreement between the simulations and the experimental data for the configurations 2 and 3, which have been obtained once again for the whole set of experiments. The results obtained for these two configurations makes it possible to obtain a correlation, given the axial coefficient as a function of the Reynolds number. Fig. 10 shows the axial coefficient dispersion versus the Reynolds number for the configurations 2 and 3. The dispersion is slightly more important for configuration 2 as expected during the visualization.

3.4. Utilization of the results for design and operating conditions

The results suggest that for tubular photoreactor, it is better to divide the inlet flow in several lateral inlets. The lateral inlet leads to a plug flow behavior and the axial dispersion is reduces by multiple inlets. When the configuration leads to a possible stagnant volume, the Reynolds number based on the internal diameter of the reactor should be higher than 4000 to supply enough energy to

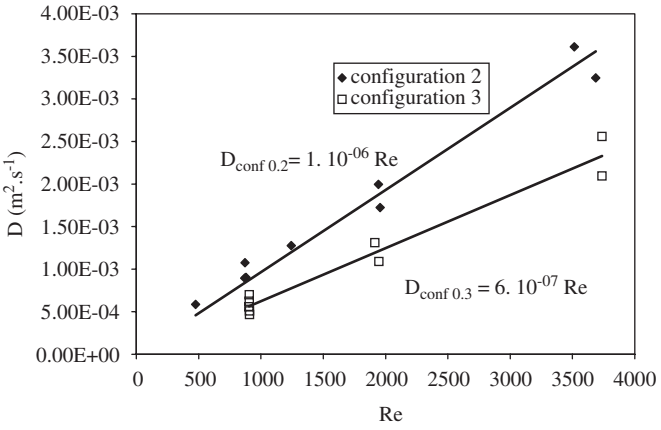

Fig. 10. Axial dispersion coefficient versus Reynolds number for the second and third configurations.

force the liquid in the whole part of the reactor even if this induces higher dispersion than with low Reynolds number. Moreover, even if it is difficult to estimate radial dispersion with RTD measurement (Legentilhomme and Legrand (1995)), colored tracer investigations showed that the radial velocity component is notable. It should be expected that all particles will receive similar quantity of radiation. This visual observation is not enough for a detailed model and radial velocity measurement. CFD simulations need to be done to validate that the amplitude of the radial component is high enough. It should be pointed out that improvements would be obtained if the inlets are in tangential positions to favor the swirling flow as proposed by Pruvost et al. (2002).

4. Conclusion

Radiotracer and colored tracer investigations were conducted in a photoreactor to study the flow behavior. Three different configurations of the inlet system have been tested to modify the RTD. The estimation of the first moments of the RTD curves showed that there is a large stagnant volume for the central inlet. It is reduced when using several lateral inlets with a Reynolds number of 4000 inside the reactor. These curves have been interpreted and simulated with appropriated compartment models. The choice of the model has been strengthened with the help of colored tracer experiments. When the inlet is located at the central bottom position, a plug flow reactor that represents the jet flow at the entrance, followed by a perfect mixer that describes the recirculation, simulates the flow behavior. The plug flow volume increases with the inlet Reynolds number. For the lateral inlet systems, the flow is well described by the plug flow with an axial dispersion model. A correlation has been determined to predict the axial coefficient as a function of the Reynolds number. The three lateral inlets configuration allows obtaining plug a flow behavior with limited axial dispersion that is the most adapted flow for better efficiency. The internal Reynolds number should be higher than 4000 to suppress possible

stagnant zones. This method does not allow predicting the radial dispersion, which is also an important parameter to assume homogeneous effect of the UV radiation, but the colored visualization seems to indicate that the radial velocity component is notable for the selected configuration. This example shows that radioactive isotopes are well-adapted tracers in the field of industrial wastewater treatment. When the knowledge of local velocities field is necessary, the colored visualization that is only accessible with a transparent mock-up can be replaced by the local wall-detector with a proper collimation system as proposed by (Thyn and Zitny (2002); Thyn et al. (2000).

Acknowledgments

The International Atomic Energy Agency, projects ARCAL LXI, RLA/8/028, whose help is greatly acknowledged, supported this work. We would like to thank Mr. Thereska (IAEA) and Mr. Jin (IAEA) for their assistances during this project and Bruno Garcia Batista for his active participation during the experiments.

References

Alves C.V.P., 2003. Scale-up and evaluation of a simple version of an ultraviolet photoreactor for the disinfection of treated wastewater. M.Sc. Thesis, Federal University of Minas Gerais, Belo Horizonte, Brazil (in Portuguese).

Andreadakis, A., Mamais, D., Christoulas, D., Kabylafka, S., 1999. Ultraviolet disinfection of secondary and tertiary effluent in the Mediterranean region. Water Sci. Technol. 40 (4–5), 253–260.

Castro Silva, J.C., 2001. Evaluation of a UV radiation photoreactor used in coliform and helminthes eggs inactivation in treated wastewaters. M.Sc. Thesis, Federal University of Minas Gerais, Belo Horizonte, Brazil.

Chernicharo, C.A.L., Daniel, L.A., Sens, M., Filho, B.C., 2001. Anaerobic reactor effluent post-treatment by means of disinfection systems. In: Chernicharo, C.A.L. (Ed.), Post-Treatment of Anaerobic Reactor Effluents, first ed. FINEP/PROSAB, Belo Horizonte, Brazil, pp. 377–454.

Claudel, S., Fonteix, C., Leclerc, J.P., Lintz, H.G., 2003. Application of the possibility theory to compartment modeling of flow pattern in industrial processes. Chem. Eng. Sci. 58, 4005–4016.

Danckwerts, P.V., 1953. Continuous flow systems, distribution of residence times. Chem. Eng. Sci. 2 (1), 1–13.

Dudukovic, M.P., 1986. Tracer methods in chemical reactors. Techniques and applications. In: Hugo I. de Lasa (Ed.), Chemical Reactor Design and Technology, NATO ASI Series.

Gonçalves, R.F., Chernicharo, C.A.L., Neto, C.O.A., Alem Sobrinho, P., Kato, M.T., Costa, R.H.R., Aisse, M.M., Zaiat, M., 2001a. Anaerobic reactor effluent by biofilm reactors. In: Chernicharo, C.A.L. (co-ordinator) Post-Treatment of Anaerobic Reactor Effluents, first ed. FINEP/PROSAB, Belo Horizonte, Brazil, pp. 171–278.

Gonçalves, R.F., Oliveira, F.F., Rubim, K.T., Cominote, M., Barbosa, E.B., Oliveira, L., Scherrer, N., Sant'anna, T.D., Souza, W.G., Passamani, F., Keller, R., Zandonade, E., 2001b. Desinfecção por radiação ultravioleta em efluentes de ETE's associando reatores UASB e biofiltros aerados submersos (Report), Universidade Federal do Espírito Santo, Vitória, Brazil.

Janex, M.L., Savoye, P., Do-Quang, Z., Blatchley, E., Laîné, J.M., 1998. Impact of water quality and reactor hydrodynamics on wastewater disinfection by UV, use of CFD modeling for performance optimization. Water Sci. Technol. 38 (6), 71–78.

Kabir, M.F., Haque, F., Vaisman, E., Langford, C.H., Kantzas, A., 2003. Disinfecting *E. coli* bacteria in drinking water using a novel fluidized bed reactor. Int. J. Chem. React. Eng. 1, A39.

Kreft, P., Scheible, O.K., Venosa, A., 1986. Hydraulic studies and cleaning evaluations of ultraviolet disinfection units. J. Water Pollut. Control Feder. 58 (12), 1129–1137.

Leclerc, J.P., Detrez, C., Antoine, B., Schweich, D., 1995. DTS: Un logiciel d'aide à l'élaboration de modèles d'écoulement. Revue de L'Institut Français du Pétrole 50, 641–656.

Leclerc, J.P., Claudel, S., Pottier, O., Lintz, H.-G., Antoine, B., 2000. Theoretical interpretation of residence time distribution measurements in industrial processes. Oil Gas Sci. Technol.—Revue de l'Institut Français du Pétrole 55 (2), 159–169.

Legentilhomme, P., Legrand, J., 1995. Distribution des temps de séjour en écoulement tourbillonnaire annulaire induit par une entre tangentielle du liquide. Can. J. Chem. Eng. 73.

Levenspiel, O., 1999. Chemical Reaction Engineering, third ed. Wiley, New York.

Liu, W., Andrews, S.A., Bolton, J.R., Linden, K.G., Sharpless, C., Stefan, M., 2002. Comparison of DBP formation from different UV technologies at bench scale. In: World Water Congress Annals, Melbourne, p. 460.

Malato, S., Blanco, J., Vidal, A., Richter, C., 2002. Photocatalysis with solar energy at pilot-plant scale: an overview. Appl. Catal. B: Environ. 37, 1–15.

Oliver, B.G., Cosgrove, E.G., 1975. The disinfection of sewage treatment plant effluents using ultraviolet light. Can. J. Chem. Eng. 53 (4), 170–174.

Pruvost, J., Legrand, J., Legentilhomme, P., 1999. Transfert photonique dans un photoréacteur à écoulement tourbillonnaire. Can. J. Chem. Eng. 77 (10), 869–876.

Pruvost, J., Legrand, J., Legentilhomme, P., Doubliez, L., 2000. Particle image velocimetry investigation of the flow-field of a 3D turbulent annular swirling decaying flow induced by means of a tangential inlet. Exp. Fluids 29, 291–301.

Pruvost, J., Legrand, J., Legentilhomme, P., 2001. Three-dimensional swirl flow velocity-field reconstruction using a neural network with radial functions. Trans. ASME 123, 920–927.

Pruvost, J., Legrand, J., Legentilhomme, P., Muller-Feuga, A., 2002. Lagrangian trajectory model for turbulent swirling flow in annular cell: comparison with residence time distribution measurements. Chem. Eng. Sci. 57, 1205–1215.

Qualls, R.G., Johnson, J.D., 1985. Modeling and efficiency of ultraviolet disinfection systems. Water Res. 9 (8), 1039–1046.

Savoye, P., Janex, M.L., Lazarova, V., 2001. Wastewater disinfection by low-pressure UV and ozone: a design approach based on water quality. Water Sci. Technol. 43 (10), 163–171.

Sahle-Demessie, E., Siefu Bekele, Pillai, U.R., 2003. Residence time distribution of fluids in stirred annular photoreactor. Catal. Today 88, 61–72.

Scheible, O.K., Bassell, C.D., 1981. Ultraviolet disinfection of a secondary wastewater treatment plant effluent. EPA 600/2-81-152, PB 81-242125, USEPA, Cincinnati.

Stegowski, Z., 1993. Accuracy of residence time distribution function parameters. Nucl. Geophys. 7 (2), 335.

Thyn, J., Zitny, R., 2002. Analysis and diagnostics of industrial processes by radiotracers and radioistope sealed sources II. CTU Faculty of Mechanical Engineering, Department of Process Engineering, Praha.

Thyn, J., Zitny, R., Kluson, J., Cechak, T., 2000. Analysis and diagnostics of industrial processes by radiotracers and radioistope sealed sources I. CTU Faculty of Mechanical Engineering, Department of Process Engineering, Praha.

USEPA—United States Environmental Protection Agency. 1986. Municipal Wastewater Disinfection-Design Manual, EPA 625/1-86/021. Cincinnati.